CHARACTERIZATION OF TRANSITION TO TURBULENCE IN SOLITARY WAVE BOUNDARY LAYER

Bambang Winarta[1], Hitoshi Tanaka[2] and Hiroto Yamaji[3]

This paper reports on continues an experimental investigation of characterizing transition to turbulence for solitary wave boundary layer in a smooth bed condition. A series of experiments have been carried out by means of a closed conduit solitary wave generation system over the Reynolds number (R_e) range 5.64 x 10^5 – 7.34 x 10^5. Additionally, the instantaneous velocities were measured by using a Laser Doppler Veloci-meter (LDV) over 50 wave numbers and at 17 to 22 points in the vertical direction. The turbulence intermittency has been analyzed based on experimental data. Moreover, momentum method has been employed for calculating bottom shear stress for all cases. And then, the turbulence intensity is plotted to give clearly description how turbulence generated in the various values of R_e. The phase difference and wave friction factor obtained from the present experiment has an excellent agreement with the result of previous studies. Inconsistency critical Reynolds number (R_{ecr}) can be found in solitary wave case in terms of phase difference and wave friction factor, this observable fact is difference with sinusoidal wave case which has consistency in R_{ecr}.

Keywords: Solitary wave; bottom boundary layer; transition to turbulence; turbulence intermittency; bottom shear stress; turbulence intensity; phase difference; wave friction factor

INTRODUCTION

Bottom boundary layer under wave motion is a key rule in sediment transport modeling for practical purposes. And by considering this fundamental importance, boundary layer problem in transition to turbulence flow will be attracting and interesting part and need much attention. Because of these reasons, many studies in both laboratory experiments and numerical has been done in the previous time. However, only several researchers have investigated boundary layer characteristics under a solitary wave motion.

Solitary wave with narrow crests without trough has been often used as an approximation of surface profile of ocean wave propagating in shoaling water area. Moreover, a tsunami wave approaching shallow water can be frequently replaced with a solitary wave. A tsunami can move a large scale of sediment deposits and bring into being a morphological change in the coastal region significantly. Investigation of flow characteristics under solitary wave motion is becoming a trending topic in the past 5 years after many large tsunamis.

Theoretical study on damping solitary wave was firstly introduced by Keulegan (1948) and then, it has been followed by some researchers in both laboratory experiment and numerical approach (e.g., Ippen and Kulin 1957; Naher 1978; Tanaka et al. 1998; Liu et al. 2006, 2007; Suntoyo and Tanaka 2009b; Sumer et al. 2010; Vittori and Blondeaux 2008, 2011). In case of laboratory experiment, Liu et al. (2006, 2007) had carried out laboratory experiment by using a wave flume facilitated by a Particle Image Velocimetry (PIV). However, their generation set-up just able to investigate boundary layer characteristics in a laminar flow and it could not do experiments in transition to turbulent flow regime. Later, Sumer et al. (2010) had accomplished a series of experiments with Reynolds number (R_e) range 2.8 x 10^4 to 2.0 x 10^6 by U-Shape oscillating water tunnel in order to observe the behavior of laminar to turbulent flow in solitary motion. Although, their experiment facility successfully to carry out solitary motion experiment in the higher Reynolds number (R_e) but it has difficulty arises in a great number of realizations required to obtain reliable ensemble averaged quantities. And by considering some problems and inconveniences faced in the previous laboratory experiment, a closed conduit generation system had been proposed and used by Tanaka et al. (2012) to conduct experiments under solitary motion. It had been followed by validation in some proper criteria. As a main conclusion, the validation results show a good agreement with the finding of past studies (Sumer et al. 2010; Vittori, G. and Blondeaux, P. 2011). The most important finding that we would like to highlight in here that a closed conduit generation system is overcoming some difficulties of experimental facilities applied in the previous studies (Liu et al. 2007; Sumer et al. 2010), particularly in achieving a reliable ensemble averaging with ease and also for conducting further experiments such as sediment transport.

[1] Civil Engineering Department, Tohoku University, 06 Aoba, Sendai, Miyagi, 980-8579, Japan
[2] Civil Engineering Department, Tohoku University, 06 Aoba, Sendai, Miyagi, 980-8579, Japan
[3] Civil Engineering Department, Tohoku University, 06 Aoba, Sendai, Miyagi, 980-8579, Japan

The present study is the next investigation of solitary wave boundary layer characteristics after successfully completion of a new generation system validation in some various criteria as given in former publication (Tanaka et al. 2012). Characterization of transition to turbulence in case of solitary wave will be an important starting point for the next experiment and investigation such as sediment transport.

THEORETICAL AND EXPERIMENTAL BACKGROUND

Solitary Wave

A solitary wave is a shallow water wave that consists of a single displacement of water above the mean water level and it is a wave of finite amplitude that propagate without change of form. The exact solution of the free stream velocity under solitary wave motion given by

$$U = U_c \sec \mathrm{h}^2(\alpha t) \tag{1}$$

where U_c is the maximum velocity under wave crest, t is the time and α is defined by

$$\alpha = a_s c = \sqrt{\frac{3H}{4h^3}}\sqrt{g(h+H)} \tag{2}$$

where c is the wave celerity, h is the water depth, H is the wave height and g is the gravitational acceleration.

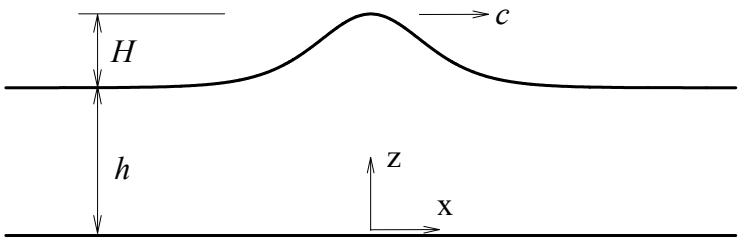

Figure 1. Sketch of a solitary wave

A Closed Conduit Generation System and Experimental Conditions

The detail explanation of generation system used in current study such as: general sketch, generation system mechanism was given in the previous publication (Tanaka et al. 2012). In the present experiments, the instantaneous velocity was measured at 17 - 22 points in the vertical direction by means of LDV and at 10ms interval over 50 wave cycles. The reason of doing measurement up to 50 wave numbers (n) is to achieve reliable ensemble averaging (Jensen et al. 1989; Sleath 1987). The current experiment conditions are summarized in **Table 1.** Reynolds number (R_e) was calculated by the following equation.

$$R_e = \frac{U_c^2}{\upsilon\alpha} \tag{3}$$

where υ is kinetic viscosity and the experimental α value was determined by fitting the exact solution of solitary wave to the measured free stream velocity.

Table 1. Experimental condition.

	T(s)	υ (cm^2/s)	U_c (cm/s)	α (s^{-1})	R_e
Case 2-2	16.90	0.0116	78.7	0.950	5.64 x 10^5
Case 2-3	15.36	0.0116	78.5	0.880	6.06 x 10^5
Case 2-4	16.99	0.0114	81.3	0.810	7.34 x 10^5

EXPERIMENTAL RESULTS

Turbulence Intermittency

The free stream velocity (U) obtained from the present experiment is compared with an exact solution for all three (3) cases shown in **Fig. 2**. A close agreement is achieved among them, although a slight discrepancy can be observed especially in the early stage of periodical motion. Due to this reason, numerical laminar is employed instead of analytical laminar solution. One important thing that we would like to emphasize in here is the negative velocity at the trailing of fluid motion inherent in a U-shape oscillating tunnel as reported by Sumer et al. (2010) can be definitely avoided.

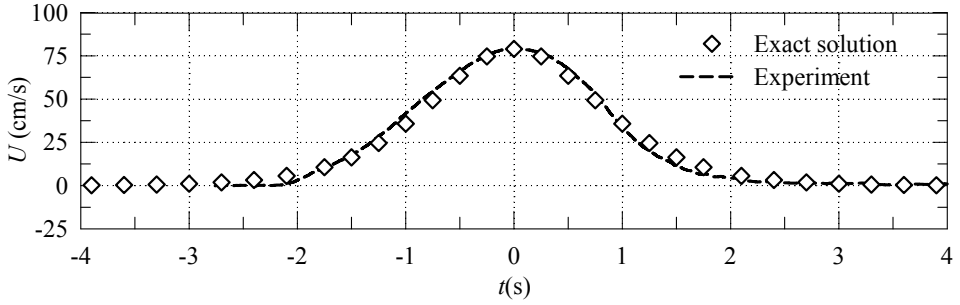

(a) Case 2-2; R_e = 5.64 x 10^5

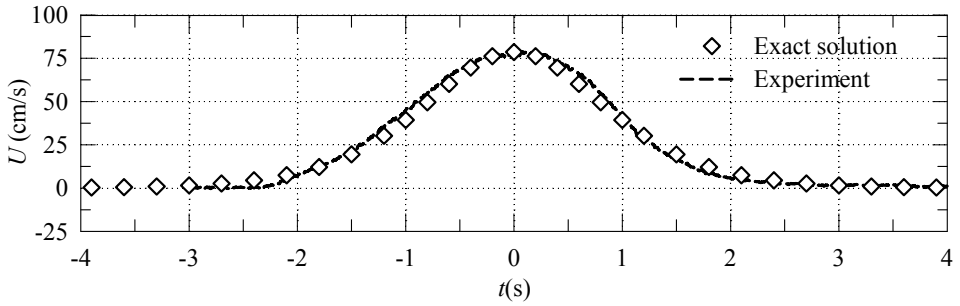

(b) Case 2-3; R_e = 6.06 x 10^5

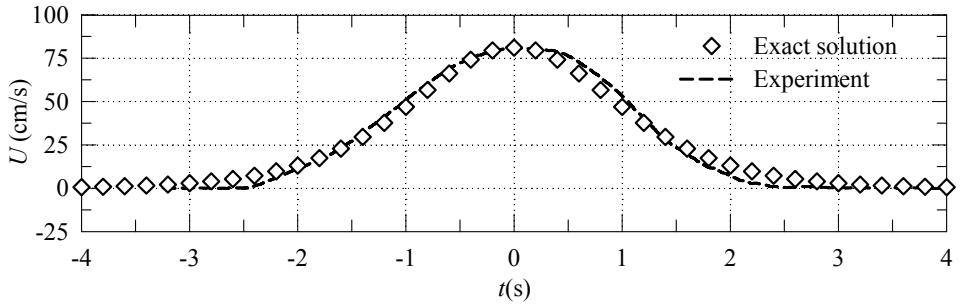

(c) Case 2-4; R_e = 7.34 x 10^5

Figure 2. Turbulence intermittency in various values of R_e

Turbulence intermittency analysis in the various values of Reynolds number (R_e) at t = 1.20s and at z = 0.049 cm, z = 0.053 cm, z = 0.052 cm for Cases 2-2, 2-3 and 2-4 respectively are depicted in **Fig. 3,** in which z is cross stream distance from the bed level and notation u is stream wise velocity. From this figure can be seen clearly dissimilar fluctuation in the different value of Reynolds number (R_e). Besides that, we can also notice how far/big the ensemble averaging result over 50 wave numbers (n) of experiment data deviates from a numerical laminar. From **Fig. 3** informs that at t = 1.20s the flow is not in laminar flow anymore but it has already moved to the higher flow regime. Moreover, it is also confirmed that deviation from numerical laminar is getting bigger by increasing Reynolds number (R_e) and it is an indication of the transition to turbulence characterization (relaminarization).

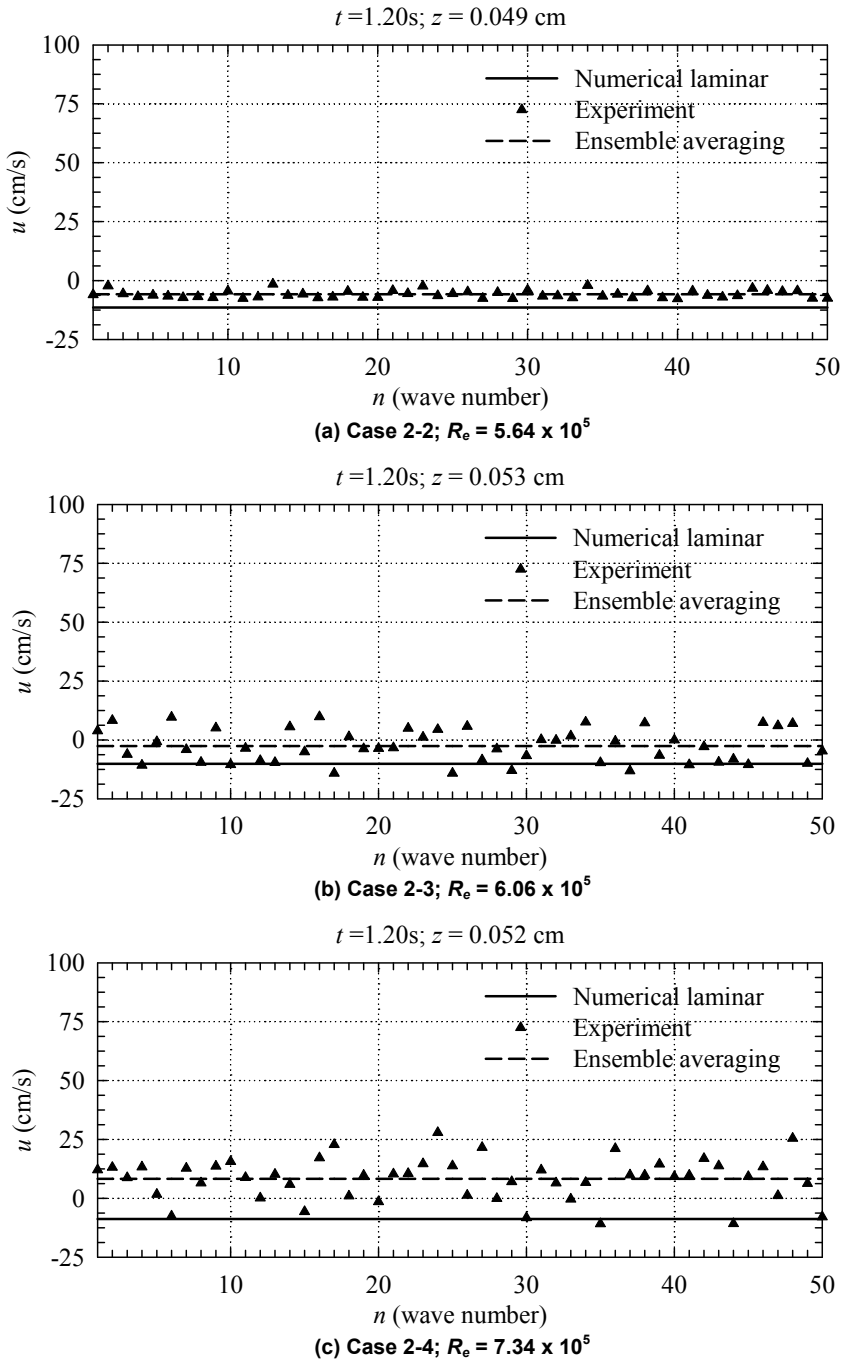

Figure 3. Turbulence intermittency in various values of R_e

Figure 4 demonstrates the distinctive feature of flow velocity at different elevation points in the vertical direction of Case 2-3, Reynolds number (R_e) = 6.06 x 10^5 at t = 1.50s. This figure illustrates how turbulent flow velocity profile built up. At z = 0.032 cm as the closest elevation point from the bottom, flow velocity deviate in higher value or magnitude than the numerical laminar computation. The deviation is getting bigger progressively in the higher elevation measurement points and achieve maximally at the measurement point z = 0.101 cm and after that, the scale of deviation is getting smaller gradually and finally over-lapping with numerical laminar at elevations z = 0.400 cm from the bottom. Then, at z higher than 0.400 cm flow velocity deviate lower than numerical laminar. Deviation with a higher value than numerical laminar in the region closed to the bottom is caused by turbulence generation. This observable fact is similar to turbulent velocity profile across a pipe flow.

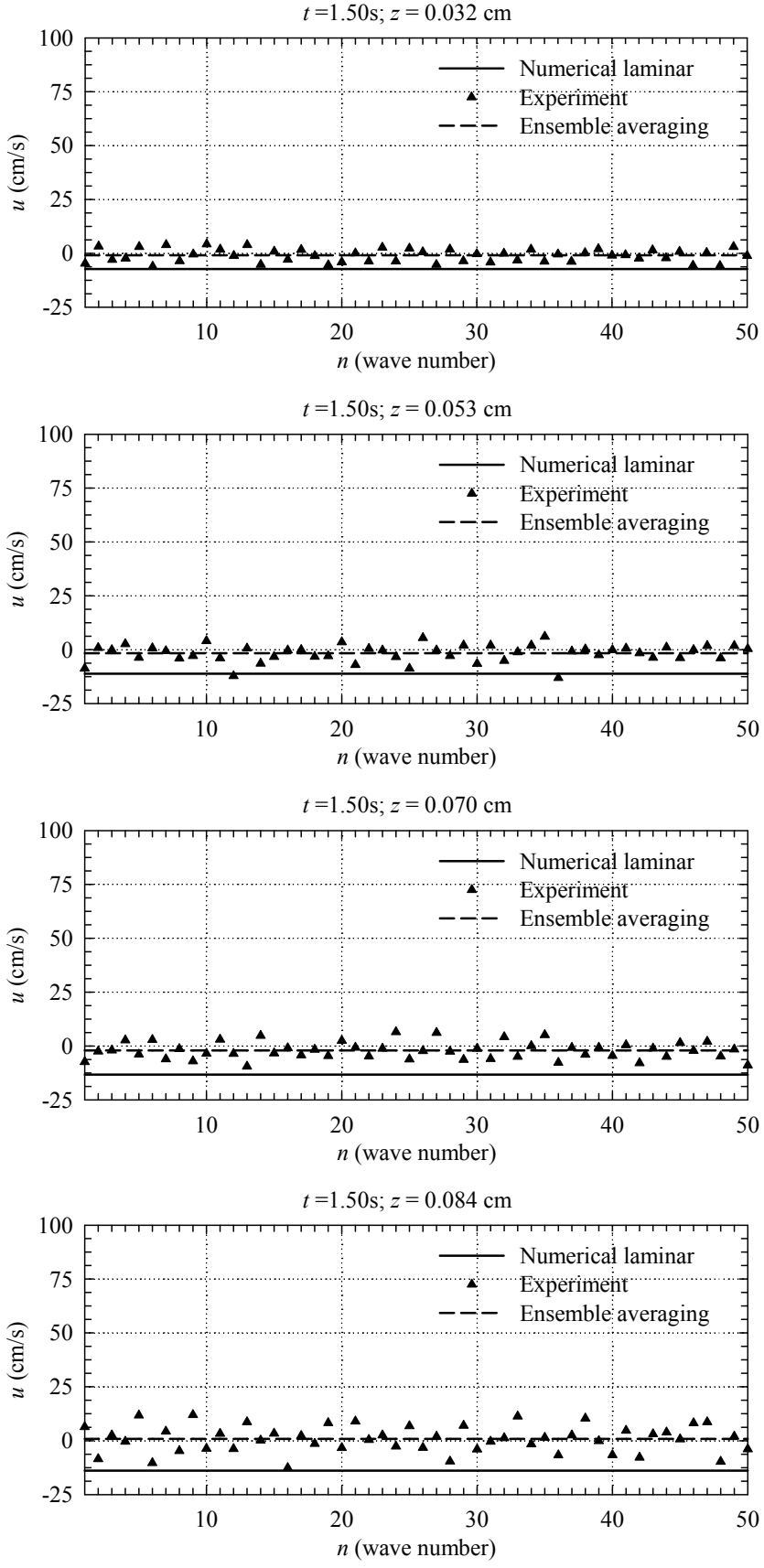

Figure 4. Intermittency in turbulent flow in the variation of measured elevations at t = 1.50s (Case 2-3; R_e = 6.06 x 10^5), continued…

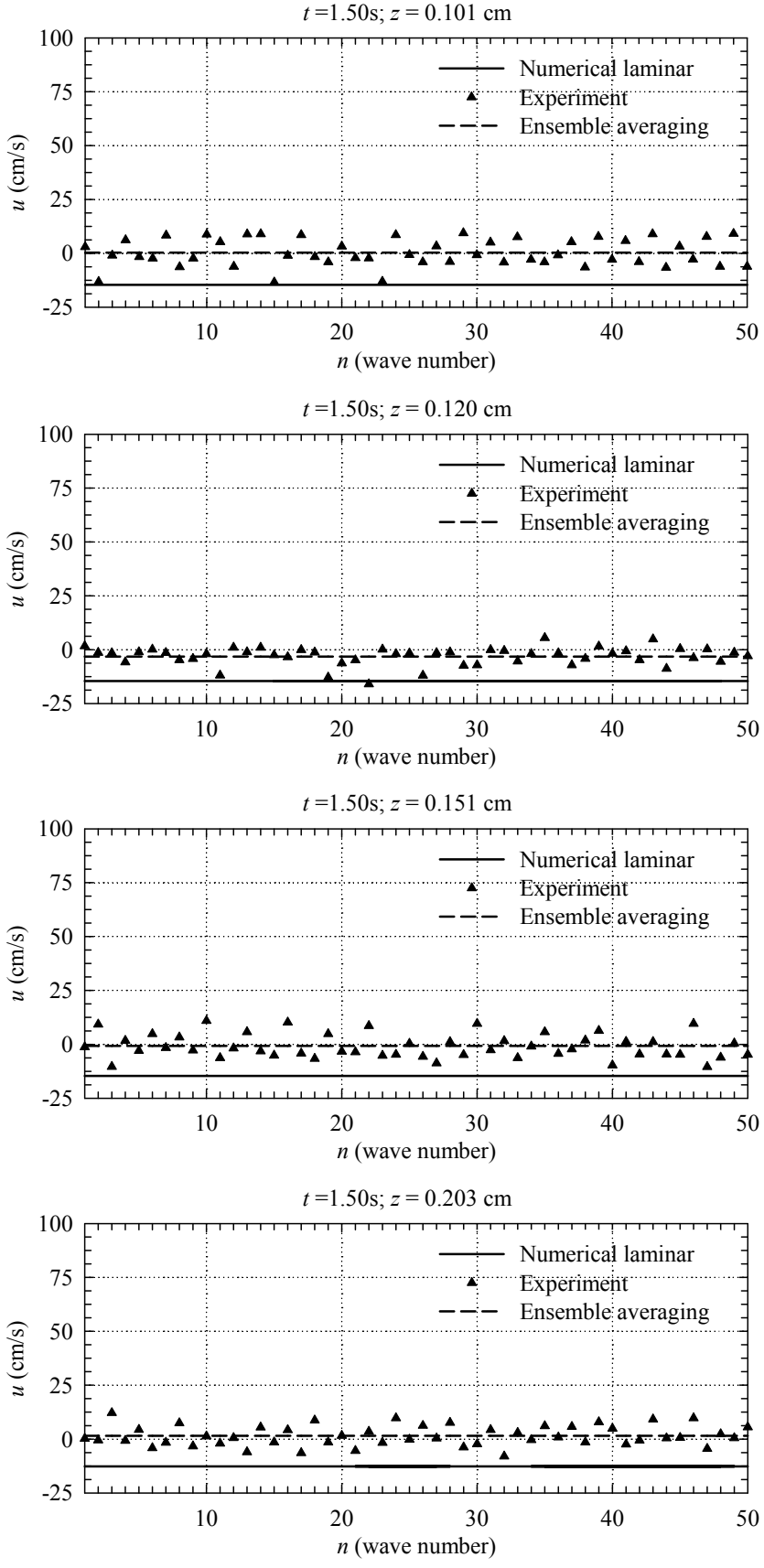

Figure 4. Intermittency in turbulent flow in the variation of measured elevations at t = 1.50s (Case 2-3; R_e = 6.06 x 10^5), continued…

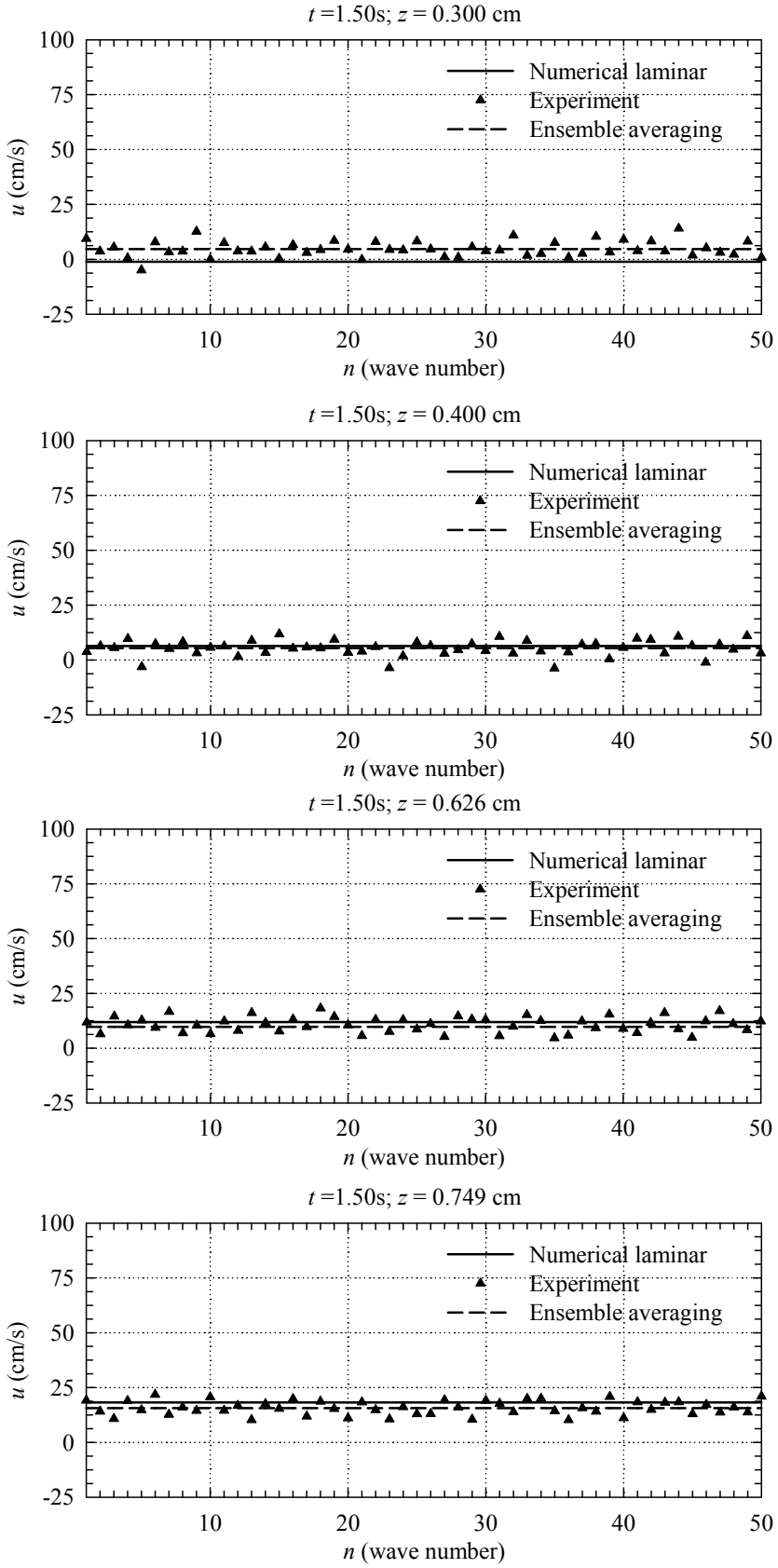

Figure 4. Intermittency in turbulent flow in the variation of measured elevations at t = 1.50s (Case 2-3; R_e = 6.06 x 10^5)

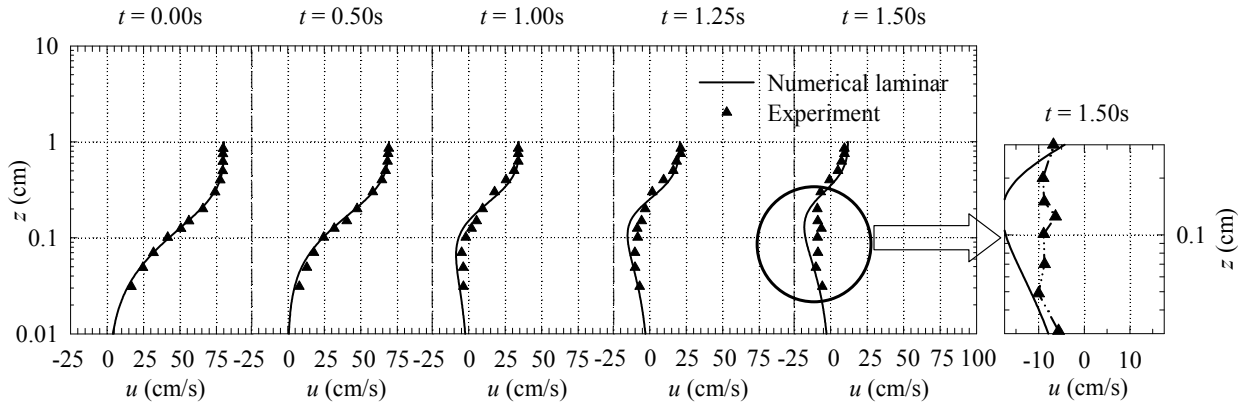

(a) Case 2-2; R_e = 5.64 x 10^5

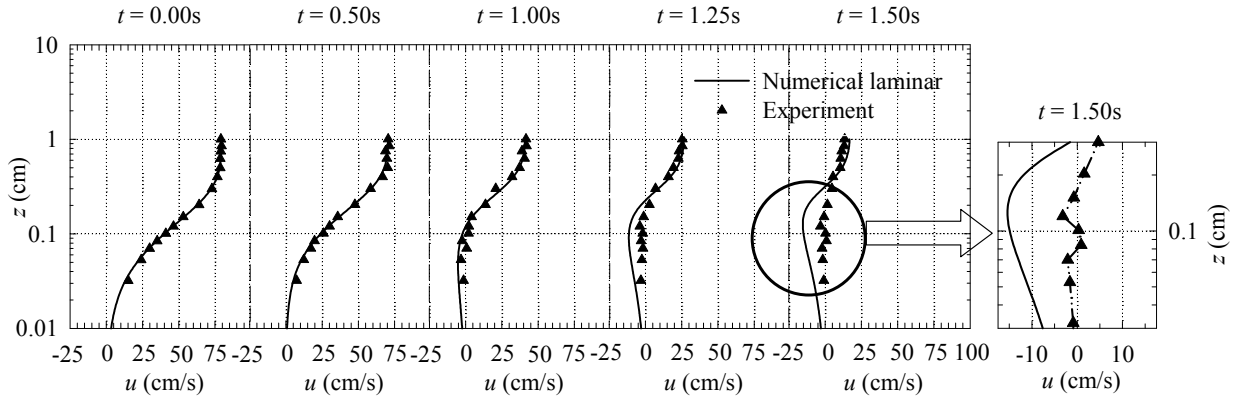

(b) Case 2-3; R_e = 6.06 x 10^5

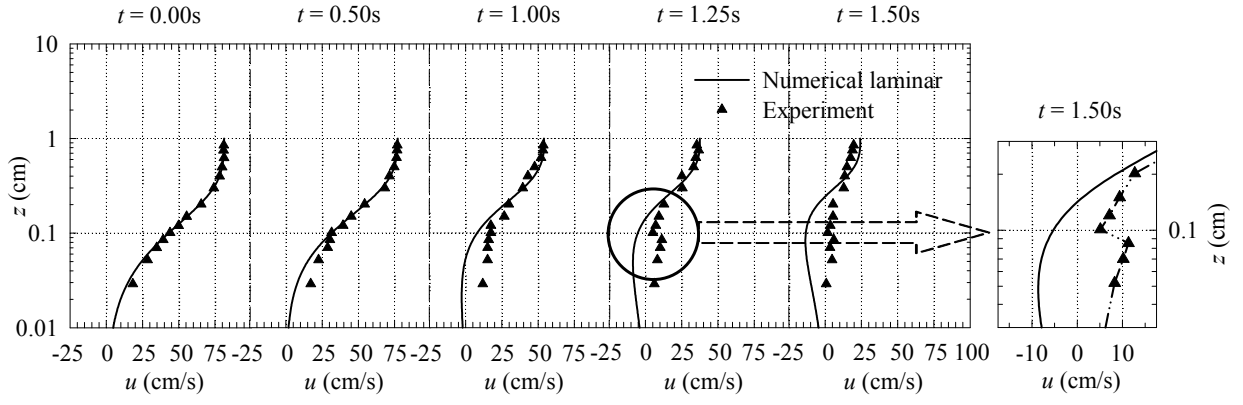

(c) Case 2-4; R_e = 7.34 x 10^5

Figure 5. The transformation of velocity profile in the variation of time in transition to turbulence flow

The transformation of flow velocity profile at Reynolds number (R_e) = 5.64 x 10^5; 6.06 x 10^5 and 7.34 x 10^5 can be seen in **Fig. 5**. This figure describes how flow velocity profiles change in the variation of time and it is started at t = 0.00s (a point of peak velocity in a solitary wave) and then, goes to decelerating phase at t = 0.50s, 1.00s, 1.25s and 1.50s. From **Fig. 5** can be seen clearly how velocity profile transforms from laminar flow to transition and next, to turbulent flow. At t = 0.00s, velocity distribution is almost has a good agreement with numerical laminar computation at Reynolds number (R_e) = 5.64 x 10^5 and 6.06 x 10^5, but a small deviation can be observed particularly in the vicinity of the bottom at Reynolds number (R_e) = 7.34 x 10^5. Then, deviation from numerical laminar occurred in

dissimilar manner for different values of Reynolds number (R_e). The velocity profile in the higher value of R_e is deviated earlier from numerical laminar computation than those in the lower value. At Reynolds number (R_e) = 5.64 x 10^5, a small deviation from numerical laminar computation can be observed particularly in the vicinity of the bottom at t = 1.00 s and then, deviation is getting bigger in the next time-variation. The deviation from numerical laminar is an indication of transition flow. An interesting fact can be found at t = 1.50s of Case 2-3, Reynolds number (R_e) is 6.06 x 10^5, in between of z = 0.101 cm and z = 0.120 cm. A discontinue in flow velocity profile can be seen at these sequent elevations. The reason why this fact occurred is in connection with turbulence intermittency as shown in **Fig. 4**. A fluctuation of flow velocity at z = 0.101 cm has magnitude range -15 cm/s to 10 cm/s, it is higher than at z = 0.120 cm with -15 cm/s to 6 cm/s. This condition produces the ensemble averaging of stream wise velocity at z = 0.101 cm is bigger than at z = 0.120 cm. The identical behavior can be found also at t = 1.25s; at Case 2-4, Reynolds number = 7.34 x 10^5 at z = 0.085 cm and z = 0.101 cm. Detail depiction in connection with this phenomenon can be seen in **Fig. 6**. As additional information, the similar flow velocity characteristic is also observed in the previous experimental studies (see figure 19, Sumer et al. 2010).

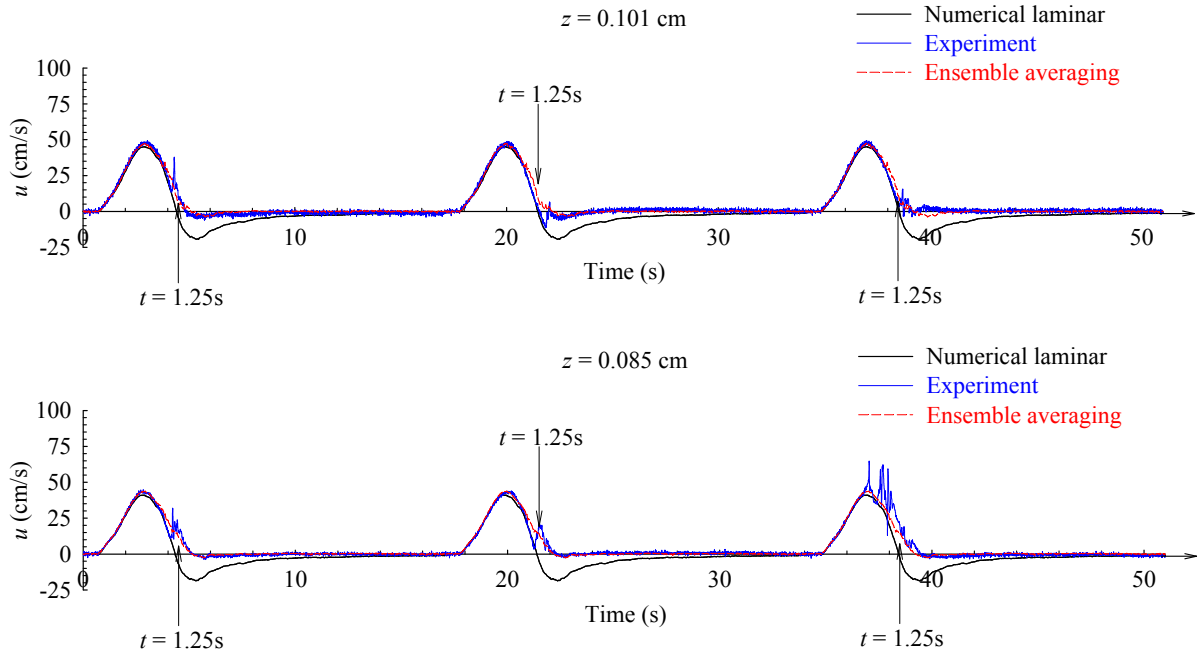

Figure 6. Instantaneous fluctuation velocity at z = 0.085 cm and z = 0.101 cm

The flow motion is sometimes turbulent and sometimes non-turbulent in the variation of time at the same elevation point (z). The quantitative descriptions of intermittency is the intermittency factor γ_i (z,t). This is defined to be γ_i = 1 for turbulent flow and γ_i = 0 for non-turbulent flow. The intermittency factor γ_i (z,t) is probability that flow at (z,t) is turbulent, defined by

$$\gamma_i(z,t) = \text{Prob}\left\{\left|u(z,t) - u_{\text{lam.}}(z,t)\right| > u'_{\text{thresh.}}(z)\right\} \qquad (4)$$

where $u'_{\text{thresh.}}$ is the thresholds of fluctuation intensity averaged during tranquil period between two peaks of "solitary-wave-like" motion.

The low levels of γ_i indicate that little such high frequency turbulence is produced and it is in this sense that the flow is laminar. **Fig. 7** shows the intermittency factor overlaid with turbulence intensity of three cases from the present experiment. It can be noticed that during accelerating phases, γ_i is equal to 0 for Case 2-2 and Case 2-3, it has tendency that the flow is laminar. A different behavior can be observed at Case 2-4 when Reynolds number (R_e) = 7.34 x 10^5, in the some time variation during accelerating phases intermittency factor has value above of 0 ($\gamma_i > 0$). This is clearly indicating of relaminarization phenomenon.

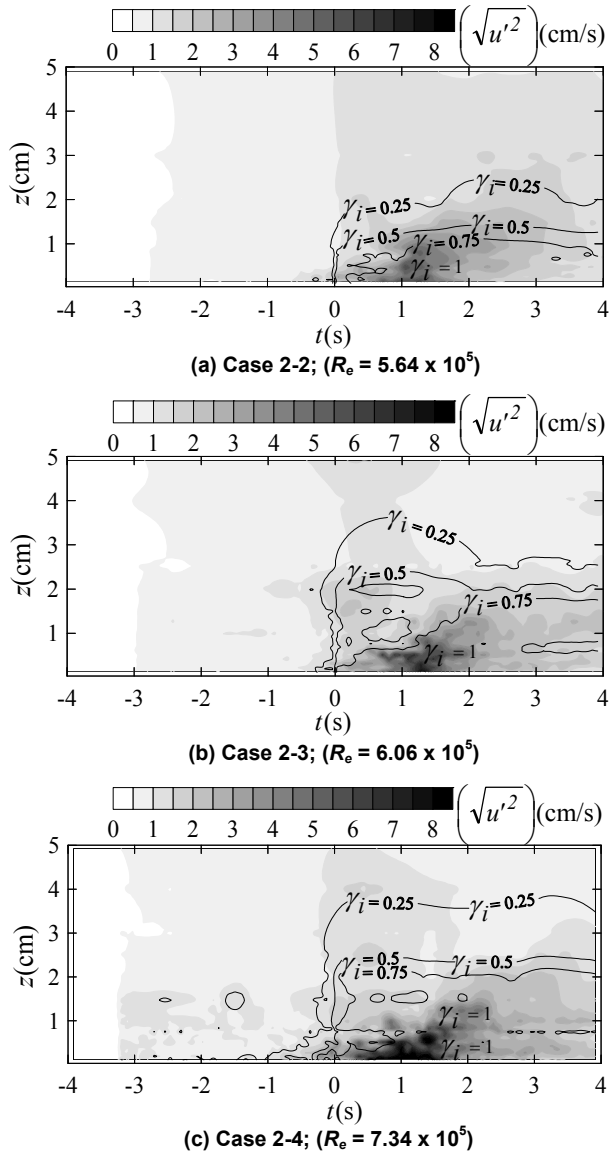

Figure 7. Intermittency in turbulent flow in the variation of measured elevations at t = 1.50s

Turbulence Intensity

The turbulence intensity (I) is defined as the ratio of the root-mean-square of the velocity fluctuations (u') to the mean flow velocity. **Figure 7** depicts out how the turbulence develops as flow progress in phase space for various value of Reynolds number (R_e). From **Fig. 7** can be seen that the turbulence intensity typically takes place in the decelerating phases but a small turbulence intensity can be found in accelerating phases at Case 2-4; Reynolds number (R_e) = 7.34 x 10^5. At t = 1s, the intensity of turbulence is high for all cases in the vicinity of the bottom and it is also fall out by high value of the intermittency factor $\gamma_i = 1$.

Bottom Shear Stress

Due to 3 cases of the present experiment is in the transition to turbulence flow regime, a momentum method is preferable used.

$$\frac{\tau_0}{\rho} = \int_0^\infty \frac{\partial(u-U)}{\partial t} dz \qquad (5)$$

where τ_0 is bottom shear stress, ρ is fluid density and U is velocity at $z = \infty$ cm or free stream velocity.

The calculation results of bottom shear stress from the present experiment by using momentum method are shown in **Fig. 8**. During the accelerating phase, bottom shear stress computed by this method agree well with the result of numerical laminar computation for R_e = 5.64 x 10^5 and 6.06 x 10^5. It has meaning that during this phase the flow condition is laminar. This is also proved by intermittency factor which equal to zero ($\gamma_i = 0$) as shown in **Fig. 7**. Deviation from numerical laminar computation in term of bottom shear stress can be observed at t = -0.2s, it come earlier than Case 2-2 which deviates from numerical laminar at t = 0s. A different behavior shown by Case 2-4; R_e = 7.34 x 10^5, deviation from numerical laminar have occurred since in the accelerating phase, it is caused by turbulence have taken place during this phase, as seen in **Fig. 7**. Deviation from numerical laminar of bottom shear stress is also an indication of relaminarization.

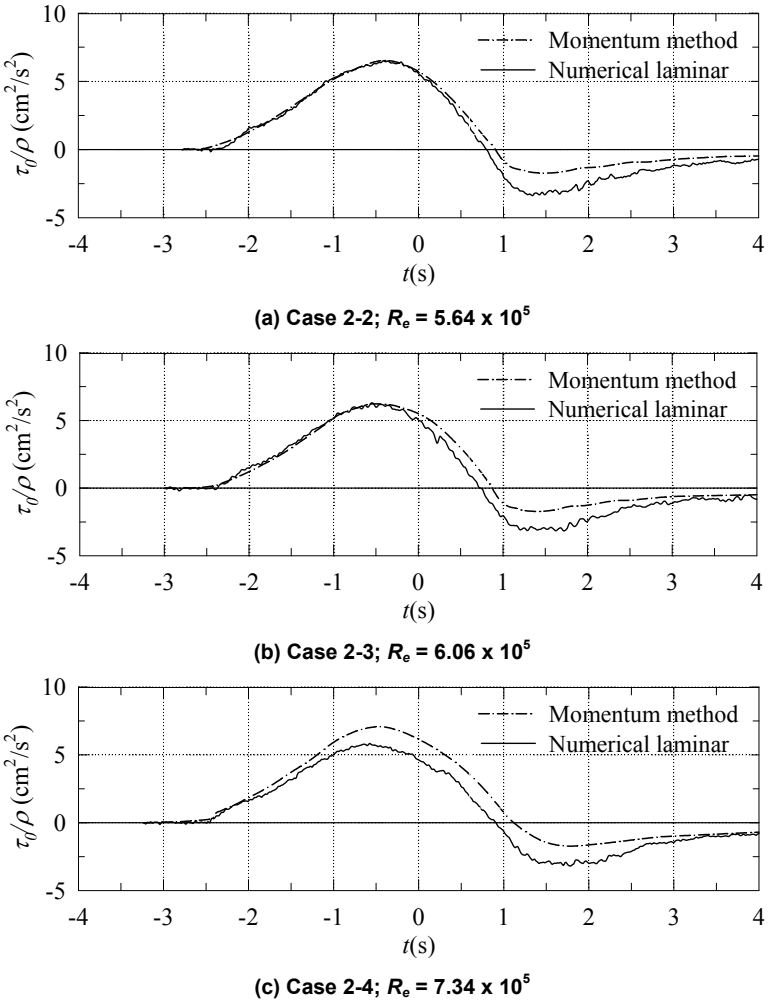

(a) Case 2-2; R_e = 5.64 x 10^5

(b) Case 2-3; R_e = 6.06 x 10^5

(c) Case 2-4; R_e = 7.34 x 10^5

Figure 8. Intermittency in turbulent flow in the variation of measured elevations at t = 1.50s

Phase Difference

Figure 9 is a phase difference between the maximum values of bottom shear stress takes place and the maximum of free stream velocity. The phase difference (θ) is calculated based on the value of Δt and α ($\theta = \Delta t\ \alpha$), where Δt is the time different between the maximum values of bottom shear stress takes place and the maximum of free stream velocity. From this figure can be seen that the phase difference obtained from the present experiment, laboratory experiment by Sumer et al. (2010) shows good agreement with the prediction of laminar theory (Liu et al. 2007) although three cases of present experiment has Reynolds number (R_e) above of critical Reynolds number at 5 x 10^5. From **Fig. 9** can be observed that deviation from the prediction of laminar theory occurs at $R_e \approx$ 1.6 x 10^5, it is based on the experimental study of Sumer et al. (2010).

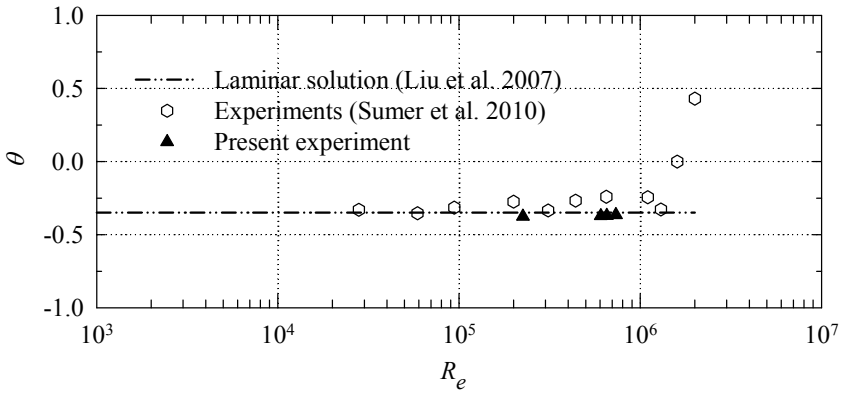

Figure 9. Intermittency in turbulent flow in the variation of measured elevations at *t* = 1.50s

Wave Friction Factor

Wave friction factor is dimensionless parameter used to estimate bed shear stress induced by wave. This parameter is related to the Shields parameter β for unidirectional current. The experimental wave friction factor can be computed by following equation from measured bottom shear stress,

$$f_w = \frac{2\tau_{0\max}}{\rho U_c^2} \tag{6}$$

where $\tau_{0\max}$ is the maximum bottom shear stress.

Analytical laminar solution for wave friction factor under solitary wave can be obtained from Keulegan (1948) and then expressed in term of Reynolds number as following equation,

$$f_w = \frac{1.71}{\sqrt{R_e}} \tag{7}$$

Vittori and Blondeaux (2011) used two (2) main dimensionless parameters in their analysis: ε and δ*, where

$$\varepsilon = \frac{H}{h} \tag{8}$$

$$\delta^* = \sqrt{2\upsilon h/\sqrt{gh}}\,/\,h \tag{9}$$

They applied Direct Numerical Simulation (DNS) and proposed heuristic law pertinent to the laminar case in the relationship between a dimensionless maximum bottom shear stress ($\tau_{0\max}^*$) and parameter ε. The empirical equation is

$$f(\varepsilon) = \tau_{0\max}^* = a_l\varepsilon^3 + b_l\varepsilon^2 + c_l\varepsilon + d_l \tag{10}$$

with $a_l = 1.698$, $b_l = -1.975$, $c_l = 0.817$ and $d_l = 0.218$

This paper is followed by the next publication on Reynolds averaged Navier-Stokes equation (RANS) modeling of the turbulent boundary layer under a solitary wave (Blondeaux and Vittori 2012). Similar to the previous publication, they also proposed the heuristic law for turbulent regime and written in the following equation:

$$f(\varepsilon) = \tau_{0\max}^* = a_t\varepsilon^3 + b_t\varepsilon^2 + c_t\varepsilon + d_t \tag{11}$$

with $a_t = 4.07$, $b_t = -4.8$, $c_t = 19.54$ and $d_t = 0.402$

The wave friction factor from the previous experiment study, DNS by Vittori and Blondeaux (2011), and RANS by Blondeaux and Vittori (2012), are plotted in similar figure with present laboratory experiment as shown in **Fig. 10.** The cases of present experiments with Reynolds number (R_e) = 5.64 x 10^5, 6.06 x 10^5 and 7.34 x 10^5 are fall in analytical laminar solution, although those cases are above of critical Reynolds number at 5 x 10^5. It is caused by transition to turbulence phenomenon happened in decelerating period, while during accelerating phase flows recover to laminar where the maximum bottom shear stress occurred. As a conclusion, wave friction factor also show an inconsistency of critical Reynolds number.

In the **Fig. 10** is also displayed turbulent prediction by using the heuristic law of Blondeaux and Vittori (2012). The wave friction factor (f_w) prediction is function of δ^*, so a different value of δ^* will give the different behaviour of wave friction factor (f_w) as displayed in the **Fig. 10**.

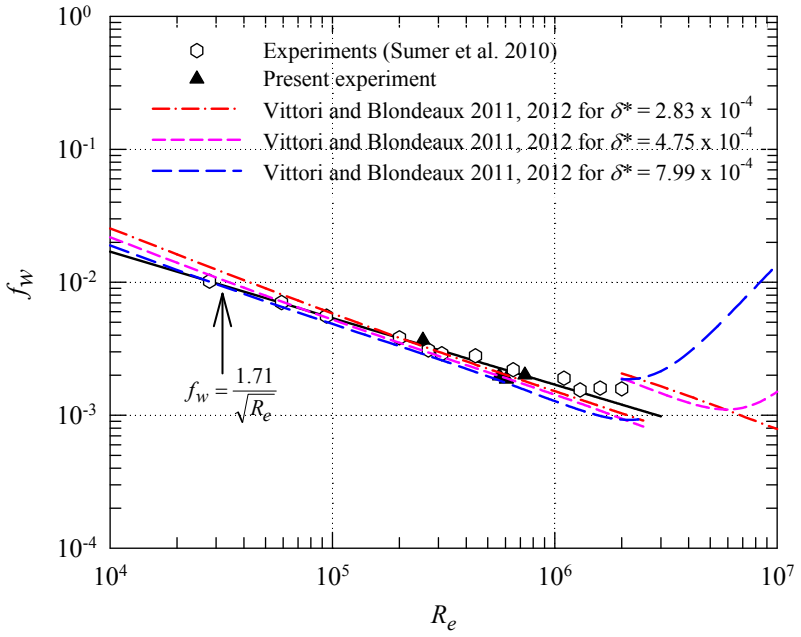

Figure 10. Wave friction factor beneath solitary wave

CONCLUSIONS

Investigation on transition to turbulence flow characteristics under solitary wave has been done based on the present experiment with various values of Reynolds number (R_e) = 5.64 x 10^5, 6.06 x 10^5 and 7.34 x 10^5 respectively. Turbulence intermittency, turbulence intensity, bottom shear stress, phase difference and wave friction factor are our concern in order to observe transition to turbulence flow behavior. The phase difference and wave friction factor obtained from the present study has a fairly good agreement with the result of previous studies. Inconsistency critical Reynolds number (R_{ecr}) can be found in solitary wave case in terms of phase difference and wave friction factor, this fact is distinct difference with sinusoidal wave case which has consistency in R_{ecr}.

ACKNOWLEDGMENTS

The laboratory experiments were conducted at Laboratory of Hydraulics, Civil Engineering Department, Tohoku University, Japan. The support from Hitachi Scholarship Foundation (HSF) for research activity of BW is also gratefully acknowledged.

REFERENCES

Blondeaux, P. and Vittori, G. 2012. RANS modeling of the turbulent boundary layer under a solitary wave. *Coastal Eng.*, 60, 1-10.

Ippen, A.T. and Kulin, G. 1957. The effects of boundary resistance on the solitary wave. *La Houille Blance*, 3, 390-407.

Jensen, B., Sumer, B.M. and Fredsøe, J. 1989. Turbulent oscillatory boundary layer at high Reynolds number. *J. Fluid Mech.*, 206, 265-297

Keulegan, G. H. 1948. Gradual damping of solitary waves. *U.S. Department of Commerce, National Bureau of Standards. RP1895*, 40, 487-498.

Liu, P. L. -F., Simarro, G., Vandever, J. and Orfila, A. 2006. Experimental and numerical investigation of viscous effectcs on solitary wave propagatation in a wave tank. *Coastal Eng.*, 53, 181-190.

Liu, P. L. -F., Park, Y. S. and Cowen, E. A. 2007. Boundary layer flow and bed shear stress under a solitary wave. *J. Fluid Mech.*, 574, 449-463.

Naheer, E. 1978. The damping of solitary waves. *J. Hydraul. Res*., 16 (3), 235-248.

Sleath, J.F.A. 1987. Turbulent oscillatory flow over rough beds. *J. Fluid Mech.*, 182, 369-409.

Sumer, B. M., Jensen, P. M., Sørensen, L. B., Fredsøe, J., Liu, P. L.-F. and Cartesen, S. 2010. Coherent structures in wave boundary layers. Part 2. Solitary motion. *J. Fluid Mech.*, 646, 207-231.

Suntoyo., and Tanaka, H. 2009b. Numerical study on boundary layer flows under solitary wave, *Journal of Hydro-Environ Res.*, 3(3), 129-137

Tanaka, H., Sumer, B. M. and Lodahl, C. 1998. Theoretical and experimental investigation on laminar boundary layers under cnoidal wave motion. *Coastal Eng.*, 40(1), 81-98.

Tanaka, H., Bambang Winarta., Suntoyo and Yamaji, H. 2012. Validation of a new generation system for bottom boundary layer beneath solitary wave, *Coastal Eng.*, 59, 46-56

Vittori, G. and Blondeaux, P. 2008. Turbulent boundary layer under a solitary wave. *J. Fluid Mech.*, 615, 433-443.

Vittori, G. and Blondeaux, P. 2011. Characteristics of the boundary layer at the bottom of a solitary wave. *Coastal Eng.*, 58, 206-213.